Neurochemistry International 127 (2019) 113–124

Contents lists available at ScienceDirect

Neurochemistry International

journal homepage: www.elsevier.com/locate/neuint

Local and systemic metabolic alterations in brain, plasma, and liver of rats in response to aging and ischemic stroke, as detected by nuclear magnetic resonance (NMR) spectroscopy

Umadevi V. Wesley[a,*,1], Vijesh J. Bhute[b,2,1], James F. Hatcher[a], Sean P. Palecek[b], Robert J. Dempsey[a]

[a] Department of Neurological Surgery, University of Wisconsin, Madison, WI, 53792, USA
[b] Department of Chemical and Biological Engineering, University of Wisconsin, Madison, WI, 53792, USA

ARTICLE INFO

Keywords:
Ischemia reperfusion
Aging
Metabolomics
Middle cerebral artery occlusion
Nuclear magnetic resonance spectroscopy

ABSTRACT

Metabolic dysfunction impacts stroke incidence and outcome. However, the intricate association between altered metabolic program due to aging, and focal ischemia in brain, circulation, and peripheral organs is not completely elucidated. Here we identified locally and systemically altered metabolites in brain, liver, and plasma as a result of normal aging, ischemic-stroke, and extended time of reperfusion injury. Comprehensive quantitative metabolic profiling was carried out using nuclear magnetic resonance spectroscopy. Aging, but healthy rats showed significant metabolic alterations in the brain, but only a few metabolic changes in the liver and plasma as compared to younger rats. But, ischemic stroke altered metabolites significantly in liver and plasma of older rats during early acute phase. Major metabolic changes were also seen in the brains of younger rats following ischemic stroke during early acute phase of injury. We further report that metabolic changes occur sequentially in a tissue specific manner during extended reperfusion time of late repair phase. First metabolic alterations occurred in brain due to local injury. Next, changes in circulating metabolites in plasma occurred during acute-repair phase transition time. Lastly, the delayed systemic effect was seen in the peripheral organ, liver that exhibited significant and persistent changes in selected metabolites during later reperfusion time. The metabolic pathways involved in energy/glucose, and amino acid metabolism, inflammation, and oxidative stress were mainly altered as a result of aging and ischemia/reperfusion. Biomarker analysis revealed citrate, lysine, and tyrosine as potential age-independent blood metabolic biomarkers of ischemia/reperfusion. Overall, our study elucidates the complex network of metabolic events as a function of normal aging and acute stroke. We further provide evidence for a clear transition from local to systemic metabolic dysfunction due to ischemic injury in a time dependent manner, which may altogether greatly impact the post-stroke outcome.

1. Introduction

Stroke is a leading cause of long-term disability and death in the United States, and about 87% of all strokes are ischemic strokes (Mozaffarian et al., 2016; Moskowitz et al., 2010; Allen and Bayraktutan, 2008). Aging, cerebral ischemia and reperfusion injury (I/R) alter the brain microenvironment including dysregulation of metabolites leading to disruption of the neuro-vascular unit and poor outcome (Kelly-Hayes et al., 2003; Bake et al., 2016; Wang et al., 2003; Cai et al., 2017; Eun et al., 2013; Bhute et al., 2017; Mauri-Capdevila et al., 2013; Jové et al., 2015; Purroy et al., 2016; Coon et al., 2006). Peripheral organ interactions following brain injury have been recently shown to affect stroke pathophysiology and outcome (Wolahan et al., 2015; Ma et al., 2015; Muscari et al., 2014). Although, the detrimental effects of these metabolic imbalances on post-stroke recovery have been recognized, our understanding of age and ischemia induced metabolic

Abbreviations: MCAO, Middle cerebral artery occlusion; SHR, Spontaneously hypertensive rats; NMR, Nuclear Magnetic Resonance Spectroscopy; I/R, Ischemia reperfusion

* Corresponding author. Department of Neurological Surgery, University of Wisconsin, Box 8660 Clinical Science Center, 600 Highland Ave; Madison, WI, 53792, USA.
E-mail address: u.wesley@neurosurgery.wisc.edu (U.V. Wesley).

[1] These authors contributed equally to this work.

[2] Present address: School of Clinical Medicine, Cambridge Institute for Medical Research, Cambridge Biomedical Campus, University of Cambridge, Cambridge, UK.

https://doi.org/10.1016/j.neuint.2019.01.025
Received 22 December 2018; Accepted 29 January 2019
Available online 30 January 2019
0197-0186/ © 2019 The Authors. Published by Elsevier Ltd. This is an open access article under the CC BY-NC-ND license (http://creativecommons.org/licenses/BY-NC-ND/4.0/).

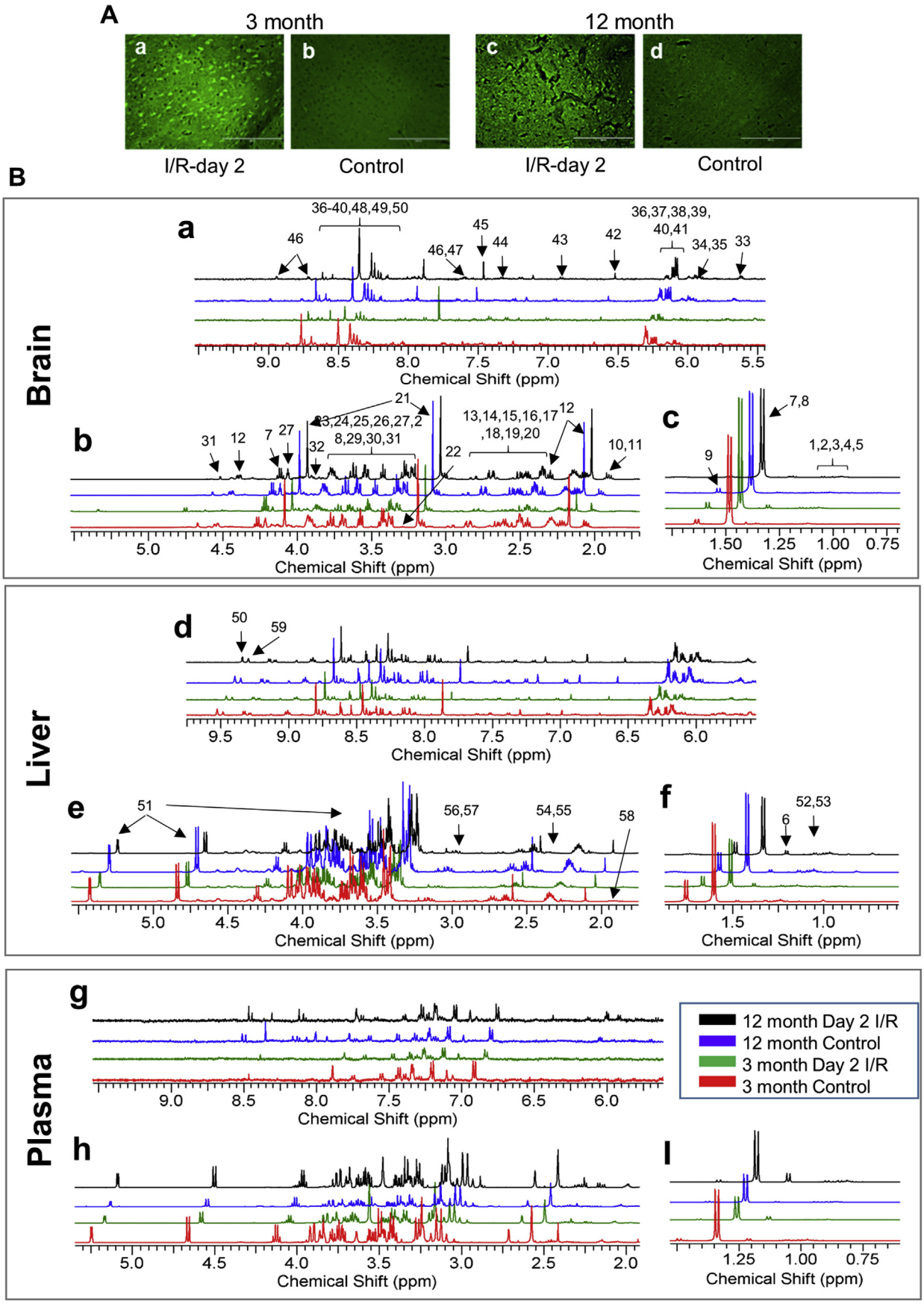

(caption on next page)

Fig. 1. Histological analysis of post-stroke infarct zone cortical sections and Representative NMR spectra.
A. Histological analysis of post-stroke infarct zone cortical sections stained with Fluoro-Jade C. Representative Fluoro-Jade C stained images showing neurodegeneration in ipsilateral region of ischemic brains at day 2 of I/R in 3 month (Aa) and 12 month old rats (Ac) as compared to control animal brains (Ab and Ad). Scale bar = 200 μM.**B.** Representative NMR spectra for the brain, liver, and plasma of 3 and 12 month old rats. **a-i.** NMR spectrum of metabolites extracted from the brain (a–c), liver (d–f), and plasma (g–i) of 3 month old control rat (red), 3 month old rat at 2 days of I/R injury (green), 12 month old control rat (blue), and 12 month old rat at 2 days of I/R injury (black). NMR spectrum is split into three regions: 5.5–9.5 ppm (a, d, g), 0.75 to 5.5 ppm (b, e, h), and 0.7–1.75 ppm (c, f, i). The arrows with numbers represent the peaks for the identified and quantified metabolites used in this study. 1: Isoleucine, 2: Valine, 3: Leucine, 4: pantothenate, 5, Isobutyrate, 6: 3-hydroxybutyrate, 7: Lactate, 8: Threonine, 9: Alanine, 10: Acetate, 11: 4-Aminobutyrate, 12: N-acetylaspartate, 13: Glutamate, 14: Glutamine, 15: Succinate, 16: Glutathione, 17: Aspartate, 18: Malate, 19: Citrate, 20: Methionine, 21: Creatine, 22: Ethanolamine, 23: O-phosphoethanolamine, 24: Choline, 25: O-Phosphocholine, 26: Glycerophosphocholine, 27: Myo-Inositol, 28: Taurine, 29: Glycine, 30: Glycerol, 31: Ascorbate, 32: Serine, 33: UDP-glucose, 34: Uracil, 34: UDP-N-Acetylglucosamine, 36: Adenosine, 37: Inosine, 38: AMP, 39: ADP, 40: ATP, 41: IMP, 42: Fumarate, 43: Tyrosine, 44: Tryptophan, 45: Chloroform (solvent), 46: Nicotinurate, 47: Uridine, 48: Hypoxanthine, 49: Formate, 50: NAD+, 51: Glucose, 52: 3-methyl-2-oxovalerate, 53: Propionate, 54: 5,6-Dihydrouracil, 55: Pyruvate, 56: O-Acetylcarnitine, 57: Beta-alanine, 58: Proline, 59: NADP+. Abbreviation: I/R: ischemia/reperfusion. (For interpretation of the references to colour in this figure legend, the reader is referred to the Web version of this article.)

changes is not complete. Thus, further systematic global or targeted analysis of metabolites in ischemic stroke context is important to better understand the disease mechanisms, and to gain insight into the drug discovery approaches to improve post-stroke outcome.

Interest in metabolomics of cerebrovascular diseases has increased tremendously in recent years as metabolites provide a functional readout of cellular biochemistry, and physiological and pathological phenotype. Metabolic profiling can lead to identification of not only biomarkers, but also disease specific pathways in plasma and tissues (Cai et al., 2017; Eun et al., 2013; Bhute et al., 2017; Mauri-Capdevila et al., 2013; Jové et al., 2015; Purroy et al., 2016; Coon et al., 2006). Nuclear Magnetic Resonance Spectroscopy (NMR) is gaining attention as a reliable technology for the study of metabolites. Indeed, NMR-based metabolomics analysis has been established successfully for biological samples, including brain tissue, plasma, urine, etc (Wen and Wong, 2017; Jung et al., 2011; Beckonert et al., 2007; Luo et al., 2016; Nagana Gowda and Raftery, 2014; Bhute and Palecek, 2015; Bhute et al., 2016; Dieterle et al., 2006).

Aging is a well-recognized risk factor for cerebrovascular disease and is associated with significant metabolic changes that influence disease incidence and outcome. Aging affects stroke outcome by increasing pro-inflammatory molecules and by impairing the anti-inflammatory system, and energy supply (Kelly-Hayes et al., 2003; Bake et al., 2016; Wang et al., 2003). Studies have demonstrated that impairment of behavioral outcomes and poorer neurological functional recovery after ischemia is more severe in middle aged rats than in younger animals (Bake et al., 2016; Wang et al., 2003; Cai et al., 2017). Epidemiological studies have revealed that human stroke occurs more often during 50–70 years of late middle age (Cai et al., 2017; Eun et al., 2013).

Emerging studies provide evidence for interactions between the brain and other peripheral organs in stroke pathophysiology. Severe brain injury resulting from stroke or trauma can lead to multiple organ dysfunction. Peripheral organs, in turn can exacerbate brain damage and affect the recovery of stroke patients (Wolahan et al., 2015; Ma et al., 2015; Muscari et al., 2014). Particularly, the liver is responsible for the synthesis and metabolism of blood coagulation factors and fibrinolytic enzymes, and indeed liver injury is reported in experimental ischemic stroke and is associated with apoptotic and inflammatory responses (Ma et al., 2015). Thus changes in metabolites of plasma, brain and those of peripheral organs may critically affect patients' ability to respond to ischemic challenges during stroke incidence and recovery. However, very little is known about the age dependent metabolic changes in post-stroke brain and peripheral organs.

The main goal of our current study is to identify the global metabolic changes associated with the advanced aging process, and cerebral ischemic injury. Here we tested our hypothesis that metabolomics profile will be altered both locally and systemically due to aging process and focal cerebral ischemia. We carried out comprehensive metabolic profiling to detect metabolites in brain, plasma, and liver as a function of aging and I/R time. Ischemic stroke was induced by middle cerebral artery occlusion. Using ^{1}H-NMR, abundant metabolites were identified and quantified at different times following reperfusion. We also identified the set of pathways and potential biomarkers associated with ischemic stroke injury. Overall, we provide evidence for the age specific metabolic alterations, and a clear transition from local to systemic metabolic dysfunction due to ischemic stroke. These studies may provide insights to further understand the metabolic mechanisms underlying aging and stroke.

2. Materials and methods

2.1. Animals

Animal housing and caring was in accordance with the NIH and ARRIVE *Guidelines for the Care and Use of Laboratory Animals*. All surgical procedures were approved by the Animal Care and Use Committee of the University of Wisconsin-Madison. We used spontaneously hypertensive rats (SHR) that provide a consistent infarction volume with a low variability. This is an approved animal model for stroke studies, as more than 70% of the patients are hypertensive. A total of 30 male Younger (3 months) and older (12 months) SHR obtained from Charles River (Wilmington, MA) were used in this study and randomly assigned to treatment groups. Investigator performing middle cerebral artery occlusion (MCAO) surgeries and euthanizing animals had no knowledge of data collection and analysis.

2.2. Focal cerebral ischemic model

Focal ischemia was induced by transient MCAO as described in our previous study (Wesley et al., 2017). Briefly, under anesthesia, a 3–0 monofilament nylon suture with a rounded tip was advanced into the left internal carotid artery lumen to block middle cerebral artery blood flow. After 1 h of occlusion, the suture was withdrawn to restore the blood flow. Sham-operated rats were subjected to the same procedures without the filament occlusion and were euthanized at day 2. Fluoro-Jade staining was used to confirm neurodegeneration in ischemic brain as previously described (Schmued and Hopkins, 2000). Briefly, brain sections were immersed in decreasing concentration of ethanol and distilled water. The slides were then immersed in a solution of 0.06% potassium permanganate ($KMnO_4$) for 15 min at room temperature and rinsed with water. Slides were then stained with 0.001% Fluoro-Jade C (Millipore) in 0.1% acetic acid for 30 min and washed with water followed by mounting. Images were taken using EVOS fluorescent microscope. For reperfusion time study, 3 month rats were euthanized at day 2, 3, 7 and 14 of I/R (n = 3 at each time point). At least three animals were used for each and this number was chosen based on the resource equation method since multiple time points are used in this study.

Aging induced metabolic changes in brain, liver, and plasma

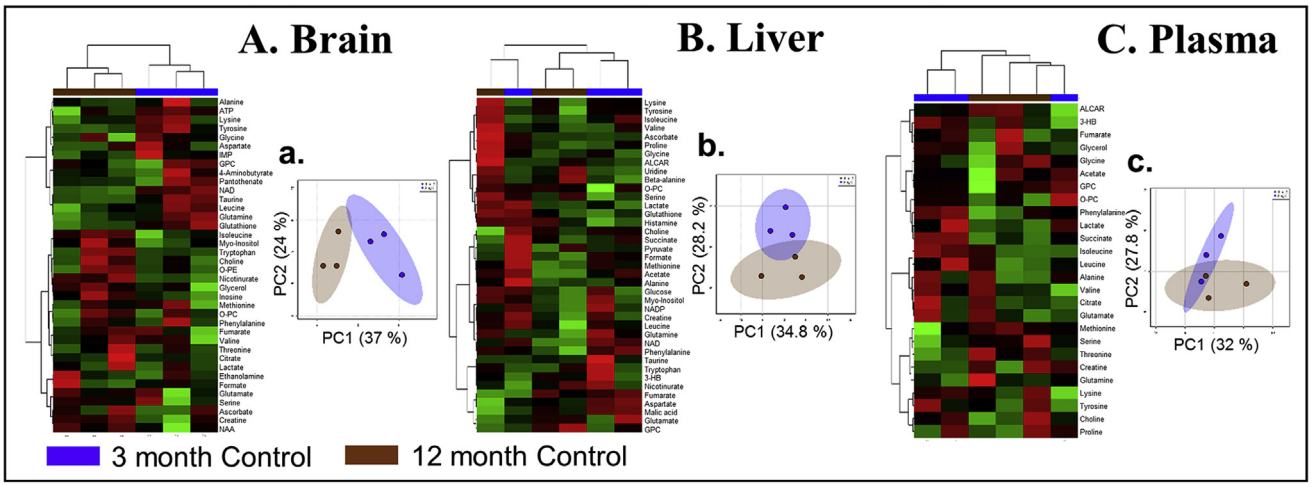

Ischemic stroke induced metabolic changes in brain, liver, and plasma (3 months rats)

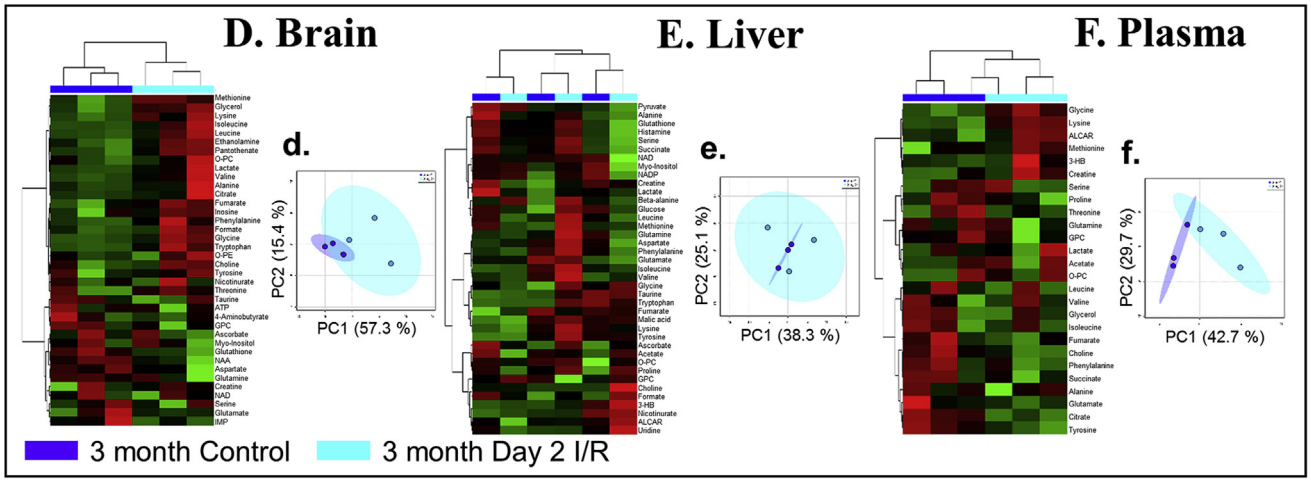

Ischemic stroke induced metabolic changes in brain, liver, and plasma (12 months rats)

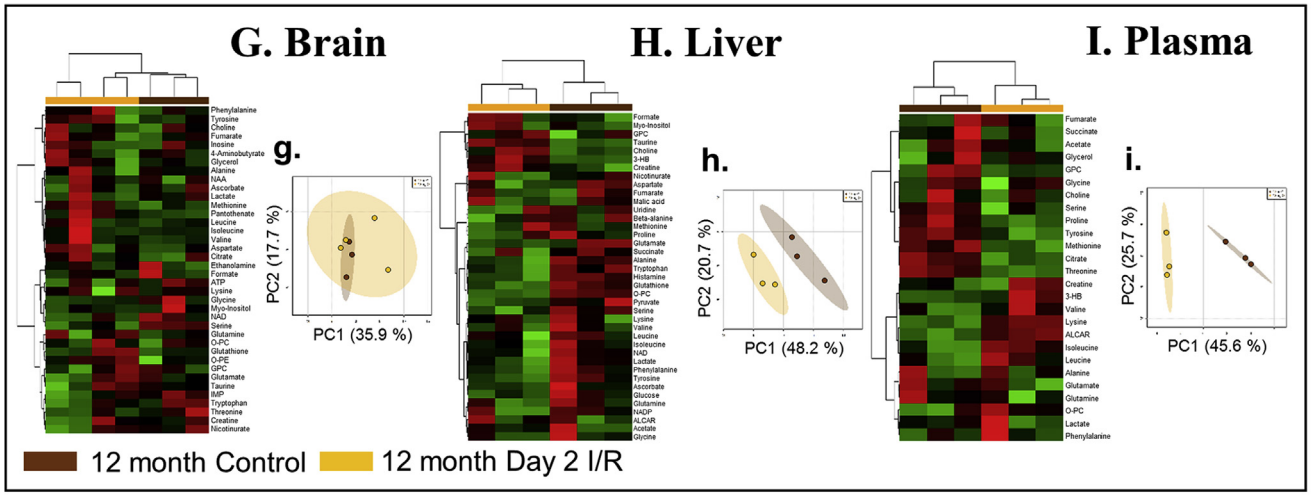

(caption on next page)

Fig. 2. Hierarchical clustering and PCA of metabolic changes induced by either aging or I/R injury in brain, liver, and plasma of 3 and 12 months old rats.
A-C. Heat maps showing hierarchical clustering of metabolic profiles of brain (A), liver (B) and plasma (C) as a function of aging (N = 3 for each group), **D-F.** Heat maps showing hierarchical clustering of metabolic profiles of brain (D), liver (E) and plasma (F) as a function of I/R injury in 3 month old (N = 3 for each group). **G-I.** Heat maps showing hierarchical clustering of metabolic profiles of brain (N = 4 for control, N = 3 for Day 2 I/R group) (G), liver (N = 3 for each group) (H) and plasma (N = 3 for each group) (I) as a function of I/R injury in 3 month old. Each row in heat map represents a metabolite
Blue - 3 month old control rat, Brown - 12 month old control rat, Cyan - 3 month old rat 2 days after I/R, Orange - 12 month old rat 2 days after I/R. **a-i.** PCA score plots for the first two principal components where each data point represents biological samples and ellipses represent 95% confidence intervals for each group. Values in the brackets on X and Y axes represent the percentage variance captured by the principal component. The analysis was performed using MetaboAnalyst. PC-Principal component. (For interpretation of the references to colour in this figure legend, the reader is referred to the Web version of this article.)

2.3. Blood plasma preparation and isolation of brain and liver tissues

Whole blood was collected into anticoagulant/EDTA -treated tubes. Plasma was isolated by centrifugation for 10 min at 2000 × *g*. The upper liquid component (plasma) was transferred into Eppendorf tubes and stored at −80 °C. Brain and liver were recovered. Cortex regions were dissected from ipsilateral and contra-lateral hemisphere of brains, quickly snap frozen in liquid nitrogen, and stored at −80° freezer.

2.4. Extraction of metabolites

Metabolites from brain and liver lysates were extracted by two phase protocol using chloroform, methanol, and water[19]. Plasma metabolites were isolated using the protocol described by Gowda and Raftery (Nagana Gowda and Raftery, 2014) using protein precipitation. Aqueous phase metabolites was dried using vacuum centrifuge at ambient conditions. Dried metabolites were reconstituted in 600 µl phosphate buffered D_2O (pH = 7) containing internal standard (0.5 mM 3-(trimethylsilyl)-2,2,3,3-tetradeuteropriopinic acid or TMSP-d4) for referencing and absolute quantification.

2.5. Metabolomics profiling using NMR

The NMR experiments and analysis was performed as described earlier (Bhute and Palecek, 2015; Bhute et al., 2016; Dieterle et al., 2006). Briefly, NMR spectra were acquired using Bruker Avance III operating at 500 MHz and temperature of 298 K. 1D spectra were acquired using standard NOESYPR1D with an acquisition time of 4 s, a mixing time of 100 ms, a relaxation delay of 1 s, and a pre-scan delay of 30 µs? Each spectrum consisted of 128 transients or free induction decays (FIDs) collected into 48 K complex data points with a spectral width of 12 ppm. Prior to Fourier transformation, the FIDs were zero-filled to 128 k data points and multiplied by an exponential window function (LB = 0.5 Hz). The chemical shifts were referenced to the TMSP peak (δ = 0 ppm), using TopSpin™ software (version 3.1, Bruker). Baseline correction and phasing was performed using ACD 1D NMR processor and the targeted profiling was performed using Chenomx NMR Profiler (Version 7.7). The concentration were normalized using probabilistic quotient normalization (Dieterle et al., 2006) and auto-scaled prior to multivariate analysis. The metabolites data are provided in the supplemental data and was uploaded to the MetaboLights server (Xia et al., 2015) (Study ID: MTBLS516).

2.6. Statistical analysis

Statistical and pathway topology analysis was performed using MetaboAnalyst 3.0[26]. We performed unsupervised clustering using principal component analysis (PCA) and hierarchical clustering on the metabolite concentrations. Pathway topology analysis was performed using the pathway analysis module on the statistically significant metabolites at different time points using global test algorithm for pathway enrichment (adjusted for multiple testing) and relative betweenness centrality to assess metabolite importance. The *Homo Sapiens* library was used for the analysis and pathways with an impact score greater than 0, false discovery rate (FDR) less than 0.05 and at least two metabolite hits were considered to be significantly affected. One way analysis of variance (ANOVA) with Tukey's HSD post hoc method was used to identify significantly altered metabolites when comparing naïve animals with I/R time. Two-tailed *t*-test was used for comparison between naïve control animals and animals with acute stroke. The data were expressed as the means ± S.D. and the *p*-values of < 0.05 was considered statistically significant. Biomarker analysis module was used to identify biomarkers in the plasma. Univariate biomarker analysis was performed on metabolic profiles. Area under the curve (AUC) in the receiver operating characteristic (ROC) curve was used to compare the diagnostic ability of metabolites to distinguish between healthy and stroke group.

3. Results

3.1. ^{1}H-NMR spectra of age and acute I/R associated metabolites in brain, liver, and plasma of rats

The induction of cerebral infarction and neurodegeneration at day 2 after 60 min of focal ischemia was confirmed by Fluoro-Jade C staining both in 3 month and 12 month old rats. Representative histological images showing ischemia induced brain damage/neurodegeneration are shown in Fig. 1**, Aa and Ac**. We then identified the age dependent changes in metabolites using 3 and 12 months SHR. Next, I/R associated metabolic changes in post-stroke SHRs were identified in acute phase at day 2 after inducing focal ischemia. Representative ^{1}H-NMR spectra of metabolites in the brain, liver, and plasma for 3 month and 12 month old rats, and 2 days after I/R injury are shown in Fig. 1B. Most of the visual peaks in the spectrum are annotated by a number that represents a metabolite (Fig. 1B) and a complete list of metabolites identified is provided in the MetaboLights database (Study ID MTBLS516).

3.2. Hierarchical clustering and PCA identified metabolic profile changes induced by either normal aging, or acute I/R

In no-stroke animals, aging alone resulted in significant metabolic changes in the brain which were evident from distinct hierarchical clustering and PCA scores plots of samples in 12 months old rats as compared to 3 months rats (Fig. 2A and a). However, in the liver (Fig. 2B and b) and plasma (Fig. 2C and c**),** the metabolic profiles of 3 month and 12 month old rats clustered together on both hierarchical clustering and PCA scores plot indicating that aging had relatively little impact on metabolites in the liver and plasma.

In stroke induced 3 month rats, I/R resulted in significant changes in metabolic profiles particularly in the brain, which was evident from hierarchical clustering of samples and PCA score plot (Fig. 2D and d). However, we observed negligible changes in the liver (Fig. 2E and e). A fewer but still significant differences in the plasma metabolic profiles were seen (Fig. 2F and f), due to I/R injury at day 2. Interestingly, in stroke induced 12 month rat brains, the metabolic profiles grouped together in both hierarchical clustering and PCA scores plot indicating that I/R injury at day 2 had minimum impact with changes in only a few metabolites as compared to no-stroke 12 month rats (Fig. 2G and g). However, I/R resulted in significant changes in metabolic profiles in the liver (Fig. 2H and h) and plasma (Fig. 2I and i) which was evident from hierarchical clustering of samples and PCA scores plots.

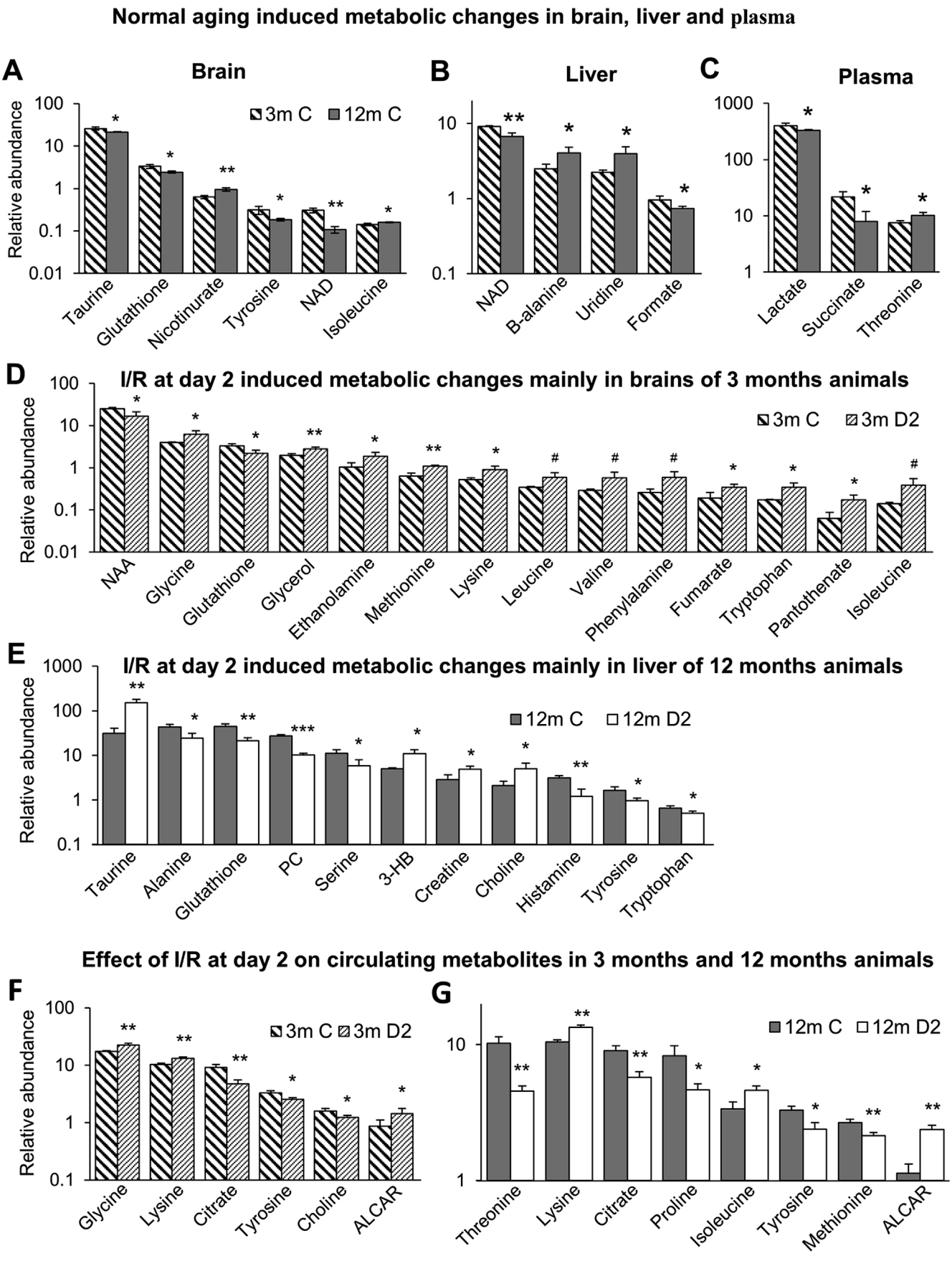

(caption on next page)

Fig. 3. Graphical representation of significant metabolic changes as a function of aging, and I/R injury in brain, liver and plasma during acute phase (2 days I/R).
A-C Bar graphs showing significantly altered metabolites due to normal aging in the brain (A), liver (B), and plasma (C).
D-E Bar graphs showing significantly altered metabolites due to I/R injury at day 2 in the brain of 3 month rats (D), and liver of 12 month (E) rats.
F-G. Bar graphs showing significantly altered metabolites due to I/R injury at day 2 on circulating metabolites in plasma of 3 month (F) and 12 month (G) rats.$^{\#}p < 0.1$, $^{*}p < 0.05$, $^{**}p < 0.01$, $^{***}p < 0.001$. Abbreviations: 3 m: 3 month old SHR, 12 m: 12 month old SHR, C: naïve, D2: 2 days after I/R injury, NAD: nicotinamide adenine dinucleotide, NAA: N-acetylaspartate, ALCAR: O-acetylcarnitine, PC: O-phosphocholine, B-alanine: beta-alanine, 3-HB: 3-hydorxybutyrate.

Table 1
Age dependent average fold changes in metabolites in response to ischemia/reperfusion (I/R) injury at day 2 in brain, liver, and plasma.

	Brain		Liver		Plasma	
	3 months I/R Vs Naïve	12 months I/R Vs Naïve	3 month I/R Vs Naïve	12 months I/R Vs Naïve	3 months I/R Vs Naïve	12 months I/R Vs Naïve
Metabolites						
Lysine	1.72↑*				1.28↑**	1.28↑***
Tyrosine				1.69↓*	1.30↓*	1.37↓*
Glutathione	1.49↓*			2.08↓**		
Tryptophan	2.00↑*			1.30↓*		
Glycine	1.58↑*				1.31↑**	
Methionine	1.72↑**					1.23↓**
Isoleucine	2.72↑#					1.37↑*
Serine		1.15↓**		1.89↓*		
Choline				2.39↑*	1.30↓*	
Citrate					1.96↓**	1.59↓**
ALCAR					1.67↑*	2.08↑**
Ethanolamine	1.81↑*					
Fumarate	1.80↑*					
Glycerol	1.45↑**					
Leucine	1.74↑#					
NAA	1.47↓*					
Pantothenate	2.75↑*					
Phenylalanine	2.25↑#					
Valine	1.97↑#					
3-HB				2.20↑*		
Alanine				1.79↓*		
Creatine				1.68↑*		
Histamine				2.63↓**		
PC				2.63↓***		
Taurine				4.97↑**		
Proline						1.79↓*
Threonine						2.22↓**

3.3. Quantification/relative abundance of altered metabolites as a function of normal aging and acute I/R

Aging process affected the relative abundance of metabolites in a tissue specific manner. Comparing to that of 3 month rats, in the brain of 12 month rats, nicotinurate and isoleucine levels were increased by 1.49 fold ($p < 0.01$) and 1.14 fold ($p < 0.05$) respectively. On the other hand, NAD (2.86 fold, $p < 0.01$), tyrosine (1.69 fold, $p < 0.05$), glutathione (1.37 fold, $p < 0.05$), and taurine (1.2 fold, $p < 0.05$) were significantly decreased (Fig. 3A). In liver of 12 month rats, NAD and formate were reduced 1.35 ($p < 0.01$) and 1.32 ($p < 0.05$) fold respectively. Whereas B-alanine and uridine were increased by 1.63 ($p < 0.05$) and 1.76 ($p < 0.05$) fold respectively (Fig. 3B).

Following stroke induction, in the brain of younger rats, 13 metabolites showed substantial changes due to I/R, out of which 10 metabolites were significantly altered ($p < 0.05$) after 2 days of I/R injury as compared to 3 month no-stroke rats (Fig. 3D). Essential amino acids showed more than 70% increase in the brain of 3 month rats. These amino acids are isoleucine (2.72 fold, $p < 0.1$), leucine (1.74 fold, $p < 0.1$), lysine (1.72 fold, $p < 0.05$), methionine (1.72 fold, $p < 0.01$), phenylalanine (2.25 fold, $p < 0.1$), tryptophan (2 fold, $p < 0.05$), and valine (1.97 fold, $p < 0.1$). Other metabolites which showed a significant increase in 3 month rats 2 days after I/R injury include glycerol (1.45 fold, $p < 0.01$), glycine (1.58 fold, $p < 0.05$), fumarate (1.8 fold, $p < 0.05$), ethanolamine, (1.81 fold, $p < 0.05$), and pantothenate (2.75 fold, $p < 0.05$). On the other hand, glutathione (1.49 fold, $p < 0.05$) and N-acetylaspartate (1.47 fold, $p < 0.05$) decreased significantly in the brain of 3 month rats (Fig. 3D). There were no significant metabolic changes in the liver of 3 month rats during acute phase of I/R injury at day 2 (Table 1).

In 12 month rats, response to I/R injury at day 2 was minimal in the brain with only one metabolite (serine, 1.15 fold, $p < 0.05$) showing significant decrease as compared to no-stroke rats (Table 1). But, the liver responded severely to I/R injury during acute phase at day 2 of I/R injury (Fig. 3E). Significantly reduced metabolites included phosphocholine (PC) (2.63 fold, $p < 0.001$), histamine (2.63 fold, $p < 0.01$), glutathione (2.08 fold, $p < 0.01$), serine (1.89 fold, $p < 0.05$), alanine (1.79 fold, $p < 0.05$), tyrosine (1.69 fold, $p < 0.05$), and tryptophan (1.3 fold, $p < 0.05$). Significantly increased metabolites were taurine (4.97 fold, $p < 0.01$), creatine (1.79 fold, $p < 0.05$), 3-hydroxybutyratre (3-HB) (1.79 fold, $p < 0.05$), and choline (1.79 fold, $p < 0.05$). Serine decreased significantly in both the brain and the liver (Fig. 3E). A comparison between the significant metabolic alterations due to I/R injury in 3 m and 12 m rats is presented in Table 1. Only those metabolites which undergo significant changes in at least one tissue or plasma in younger or 12 m old rats after 2 days of I/R injury are shown.

3.4. Normal aging process and acute I/R alter circulating blood metabolites

Since secreted metabolites can critically impact stroke outcome, we further determined the effects of either aging or stroke on the circulating metabolites in the plasma of 3 and 12 month old rats. Aging significantly decreased the levels of succinate (2.7 fold, $p < 0.05$) and lactate (1.22 fold, $p < 0.05$), and significantly increased threonine (1.36 fold, $p < 0.05$) (Fig. 3C).

In focal ischemia induced animals, three sets of altered metabolites were identified. First, metabolites altered due to I/R in the plasma of both young and old animals included lysine (3 month: 1.28 fold, $p < 0.01$; 12 month: 1.28 fold $p < 0.001$) and o-acetylcarnitine (ALCAR) (3 month: 1.67 fold, $p < 0.05$; 12 month: 2.08 fold, $p < 0.01$) that were significantly increased, and citrate (3 month: 1.96 fold, $p < 0.01$; 12 month: 1.59 fold, $p < 0.01$) and tyrosine (3 month: 1.3 fold, $p < 0.05$; 12 month: 1.37 fold, $p < 0.05$) that were significantly decreased (Fig. 3F and G). Second, metabolites affected due to I/R only in the plasma of 3 month rats included choline that was decreased 1.3 fold, $p < 0.05$, and glycine that was increased 1.31 fold, $p < 0.01$ (Fig. 3F). Third, metabolites affected due to I/R only in plasma of 12 month rats included threonine (2.22 fold, $p < 0.05$), proline (1.79 fold, $p < 0.05$), and methionine (1.23 fold, $p < 0.01$) that were significantly decreased, and isoleucine (1.37 fold, $p < 0.05$) that was significantly increased 2 days after I/R injury (Fig. 3G).

3.5. Extended ischemia/reperfusion time significantly impacts metabolic changes in brain, liver, and plasma

Time of re-perfusion after ischemia strongly affects the efficacy of treatments and stroke recovery. Hence, we next examined if extended time of I/R impacts metabolic levels in brain, liver, and plasma of 3 month rats, as these younger rats sustain ischemic injury for a longer period.

We examined the metabolic changes in brain, liver, and plasma at day 2, day 3, week 1, and week 2 of re-perfusion time. Early, mid and

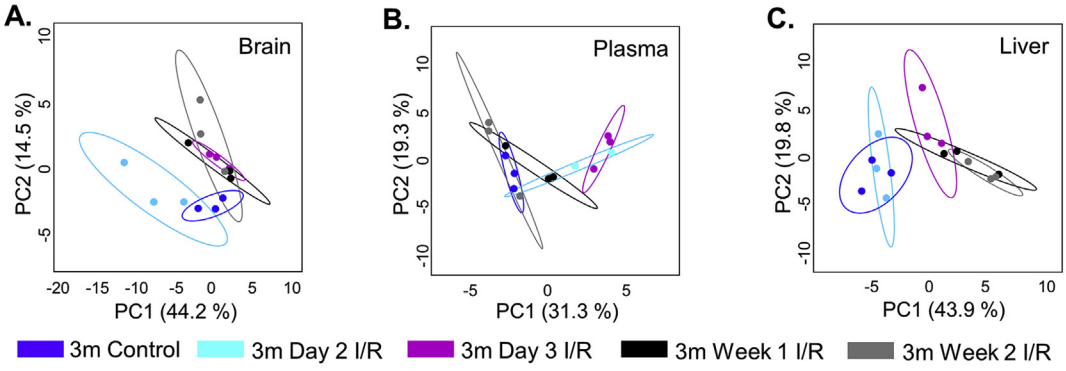

D

Metabolic Pathways (Early phase)	2 days post I/R in brain		
	# metabolites	p value	Impact
Cysteine and methionine metabolism	2	4.48E-03	0.045
Lysine degradation	2	9.32E-03	0.147
Aminoacyl-tRNA biosynthesis	8	1.15E-02	0.056
Glutathione metabolism	2	1.70E-02	0.237
Alanine, aspartate and glutamate	2	2.42E-02	0.003
Pantothenate and CoA biosynthesis	2	3.69E-02	0.18
Glycine, serine and threonine	2	3.81E-02	0.188
Phenylalanine metabolism	2	3.86E-02	0.119
Phenylalanine, tyrosine and tryptophan biosynthesis	2	4.52E-02	0.001

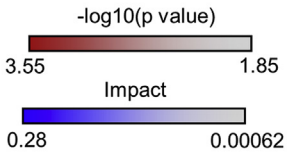

E

Metabolic Pathways (Late phase)	2 weeks post I/R in liver		
	# metabolites	p value	Impact
Pyridine metabolism	2	2.79E-04	0.021
Glutathione metabolism	2	5.39E-04	0.249
Nicotinate and nicotinamide	3	5.84E-04	0.002
Alanine, aspartate and glutamate	3	1.31E-03	0.207
Propanoate metabolism	2	1.81E-03	0.001
Sulfur metabolism	2	2.53E-03	0.033
Cysteine and methionine metabolism	4	3.21E-03	0.074
Phenylalanine metabolism	4	3.60E-03	0.119
Tyrosine metabolism	3	3.62E-03	0.047
Pyruvate metabolism	2	4.80E-03	0.282
Glycolysis or Gluconeogenesis	2	4.80E-03	0.096
Taurine and hypotaurine metabolism	2	4.80E-03	0.022
Arginine and proline metabolism	3	5.24E-03	0.032
Valine, leucine and isoleucine synthesis	4	7.47E-03	0.061
Aminoacyl-tRNA biosynthesis	8	1.06E-02	0.056
Citrate cycle (TCA cycle)	2	1.14E-02	0.105
Butanoate metabolism	2	1.14E-02	0.103
Phenylalanine, tyrosine and tryptophan	2	1.15E-02	0.008
Glycine, serine and threonine metabolism	3	1.18E-02	0.137
Valine, leucine and isoleucine degradation	3	1.40E-02	0.022

Fig. 4. Extended time of I/R injury during late phase significantly impacts metabolic levels in brain, liver, and plasma of 3 month old rats (N = 3 per group).
A-C. Scores plot of first two principal components from PCA of metabolic profiles for brain (A) plasma (B), and liver (C). Each data point represents biological samples and ellipses represent 95% confidence intervals for each group. Color code for time points: blue- Naïve Control, cyan-2 days I/R, magenta-3 days I/R, Black-1 week I/R and grey-2 weeks I/R. The analysis was performed using MetaboAnalyst.
D and E. Metabolic pathways which are significantly enriched in the brain of 3 month rats during early phase at day 2 of I/R injury (D) and liver of 3 month rats during late phase at 2 weeks after I/R injury (E). Pathways are considered significantly enriched if $p < 0.05$, impact > 0 and number of metabolite hits in the pathway > 1. Impact score indicates the impact of significantly affected metabolites in the pathway based on network topology measure of relative betweenness centrality. (For interpretation of the references to colour in this figure legend, the reader is referred to the Web version of this article.)

late metabolic changes occurred in a time and tissue specific manner. Early response was seen in brain, as the metabolic changes were prominent at day 2 of I/R. However, at later time points brain showed metabolic profiles that were similar to no-stroke animals as indicated by the hierarchical clustering, and PCA (Fig. 4A). Mid-response was observed in plasma. Significant changes in plasma metabolites were seen starting at day 2 which lasted until week 1 after I/R injury. Metabolite levels were back to no-stroke animal levels after 1 week of I/R, indicating alterations in secreted metabolites during the acute to early repair phase (Fig. 4B). Late metabolic responses were observed in liver which elicited significant metabolic changes starting from day 3 of I/R which continued to remain altered until 2 weeks of I/R (Fig. 4C). A complete list of significantly affected metabolites with fold changes is shown in Supplementary Table 1 and a graphical representation for these changes is shown in Supplementary Fig. 1.

We next performed pathway topology analysis to identify metabolic pathways that were affected in the brain (Fig. 4D), particularly at day 2 after I/R injury, and week 2 after I/R injury in the liver (Fig. 4E), as these time points showed significant metabolic changes in these two organs. Lysine degradation and pantothenate and CoA biosynthesis pathways were enriched only in the brain at day 2 after I/R injury (Fig. 4D). At week 2 of I/R, the liver showed significant enrichment of pathways involved in pyrimidine metabolism, nicotinate and nicotinamide metabolism, propanoate metabolism, sulfur metabolism, tyrosine metabolism, pyruvate metabolism, glycolysis or gluconeogenesis, taurine and hypotaurine metabolism, arginine and proline metabolism, valine, leucine and isoleucine metabolism, butanoate metabolism, and citric acid cycle (Fig. 4E). Specific pathways involved in glutathione metabolism, glycine, serine and threonine metabolism, phenylalanine metabolism, cysteine and methionine metabolism, alanine, aspartate and glutamate metabolism, and aminoacyl tRNA biosynthesis (or protein synthesis) were altered in both liver and brain (Hits > 1, Impact > 0 and $p < 0.05$) (Fig. 4D and E).

3.6. Biomarker analysis reveals potential blood metabolic markers of I/R in plasma of rats

Using univariate biomarker and the ROC curve analysis, we examined if metabolic profiles of plasma obtained from stroke induced rats at day 2 after I/R injury can identify potential circulating biomarkers independent of age (N = 6 for control and N = 6 for day 2 after I/R). The results from ROC curve analysis with a cut-off of

A

Metabolites	AUC	95% CI	p value	Fold change
Citrate	1.00	(1-1)	1.35E-05	1.74 ↓
Lysine	1.00	(1-1)	1.10E-06	1.28 ↑
Tyrosine	1.00	(1-1)	8.13E-05	1.34 ↓
ALCAR	0.94	(0.78-1)	4.50E-03	1.90 ↑
3-HB	0.92	(0.67-1)	1.86E-02	2.70 ↑
Threonine	0.92	(0.67-1)	6.25E-03	1.54 ↓
Proline	0.89	(0.58-1)	1.04E-02	1.44 ↓

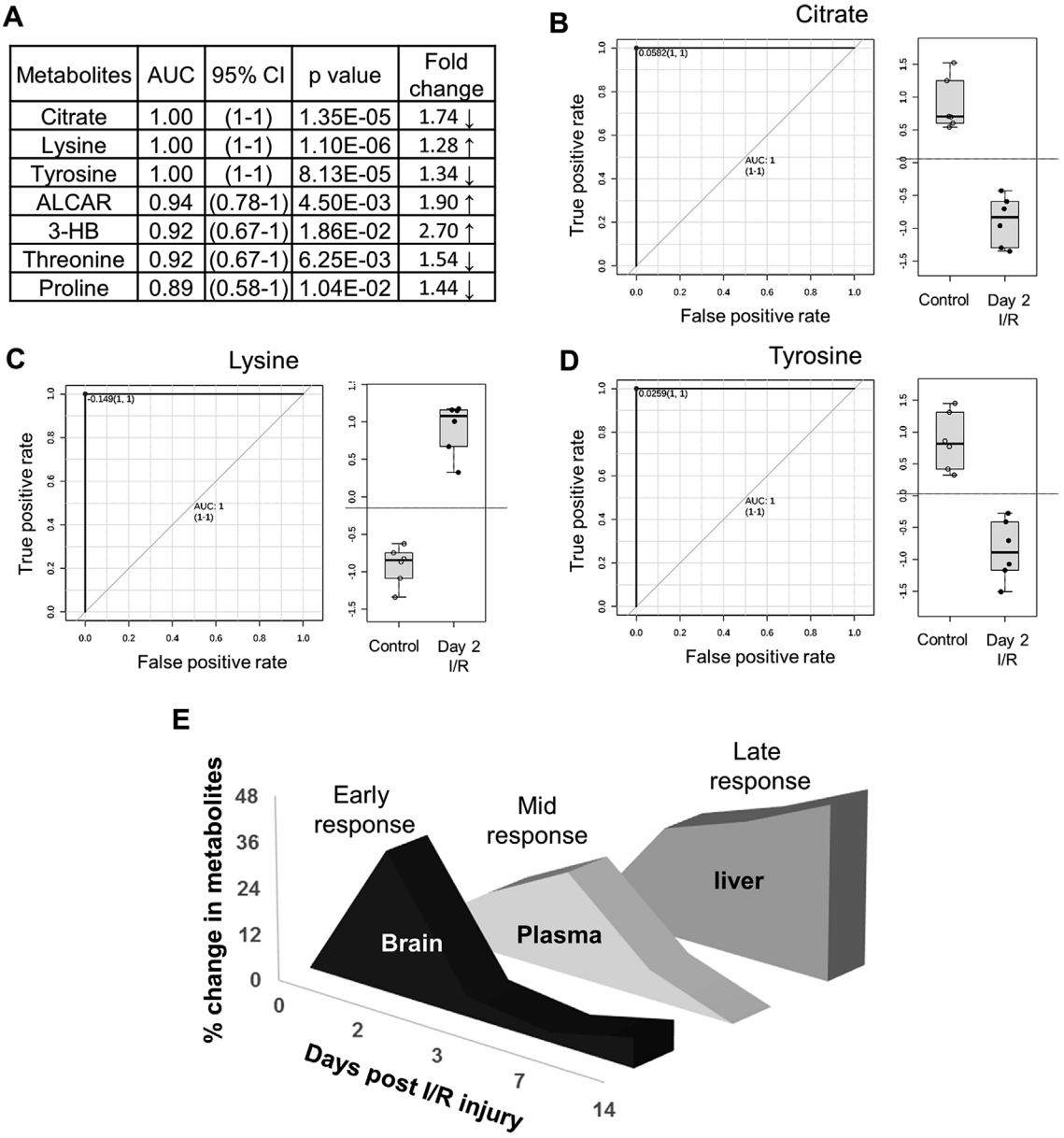

Fig. 5. Biomarker analysis reveals potential metabolic markers of I/R in plasma of rats.
A. Results from univariate biomarker analysis are shown for metabolites with $p < 0.05$ in plasma at 2 days of I/R injury in rats irrespective of their age. **B, C, D.** Receptor operative characteristic (ROC) curves for the top three metabolites which showed area under the curve (AUC) of 1 include Citrate (B), lysine (C), and tyrosine (D). **E.** Schematic presentation of percent metabolic changes affected by the time of I/R injury in brain, liver, and plasma of 3 month old rats. X-axis represents days post I/R injury and Y-axis represents the percentage of metabolites that showed significant changes relative to respective control tissues or plasma at a given time point. CI: confidence interval, ALCAR: O-acetylcarnitine, 3-HB: 3-hydroxybutyrate.

$p < 0.05$ is shown in Fig. 5A. ROC curve analysis was performed to visualize the accuracy of predictions where y-axis represents the true-positive rate (sensitivity) and x-axis represents false-positive rate (1-specificity) associated with a particular test value. Area under curve (AUC) metric indicated high sensitivity and specificity for citrate, lysine, and tyrosine in their ability to differentiate between no-stroke animals and focal ischemia/stroke induced animals irrespective of the age of rats (Fig. 5B, C, and 5D).

An overall schematic summary of the sequential metabolic responses as a function of reperfusion time in brain, plasma, and liver of 3 month rats is shown in Fig. 5E.

4. Discussion

Despite the clinical significance of post-stroke metabolic changes, a detailed analysis of local and systemic effects of aging process and stroke on metabolism has not been well documented. In this comprehensive study using the rat MCAO stroke model and NMR spectroscopy approach, we have identified differential metabolic responses due to normal aging, acute ischemic stroke, and extended reperfusion time, and provide evidence for local and prolonged systemic effects of stroke on metabolism, particularly in brain, liver, and blood plasma. These data point to a potential role for not only local, but also systemic effects of cerebral ischemia.

First, we examined the impact of aging process on metabolic profiles using two age groups, 3 month and 12 month old rats. SHR rats show accelerated aging signs such as brain atrophy, and vascular dementia, and most of them are known to live only up to 15–17 months. Hence 12 months SHR rats are generally considered middle age – early old age. In humans, this age group is considered as important for stroke incidence.

Therefore we used 12 months old rats to represent older age group. We identified that advancing of normal aging process from 3 m to 12 m causes significant metabolic changes in a tissue dependent manner, with a higher number of changes occurring in brain followed by plasma and liver. Of note, in 12 m rats, Nicotinamide adenine dinucleotide (NAD) was reduced significantly in both brain and liver. NAD is involved in maintaining redox status, and redox imbalance is a hallmark event in the pathophysiology and prognosis of stroke (Ye et al., 2016). Being the major energy fuel of the cell, NAD serves as the substrate to several enzymes including poly (ADP-ribose) polymerase (PARP) that induces apoptosis and inflammation (Ma et al., 2012; Braidy et al., 2011; Massudi et al., 2012). Consistent with our data, NAD is shown to be decreased with age in tissues from wistar rats (Braidy et al., 2011) and humans (Massudi et al., 2012). Interestingly, an anti-oxidant glutathione, and tyrosine, a precursor of catecholamines were also reduced in the brain of 12 m rats. Indeed, catecholamines have been shown to be depleted with aging in different parts of brain (Kim et al., 2017; Ponzio et al., 1982) likely due to reduced activity of tyrosine hydroxylase enzyme. This may have implications in disrupted brain functions.

It is increasingly evident that the peripheral organs distant from the brain are also involved in the regulation of multiple metabolic pathways, and immune-inflammatory axes that impact stroke incidence and outcome (Wolahan et al., 2015; Ma et al., 2015; Muscari et al., 2014). In addition to brain, the liver of 12 m animals also showed decreased NAD levels (Simpkins et al., 1977). Liver is responsible for the synthesis and metabolism of blood coagulation factors and fibrinolytic enzymes associated with pathophysiology of stroke (Wolahan et al., 2015; Ma et al., 2015). Importantly, liver injury is reported in experimental ischemic stroke and is associated with apoptotic and inflammatory responses. We further identified significantly lower levels of circulating succinate and lactate, and higher levels of threonine in the plasma of aged animals. Decreased succinate has been observed in urine from patients with Crohn's and inflammatory bowel disease (Connolly and Duley, 1999). Interestingly, succinate is associated with ATP formation and is an intermediate in the tricarboxylic acid (TCA cycle). Its dysregulation affects processes such as gene expression, inflammation, tissue repair, and angiogenesis (Schicho et al., 2012), an integral part of post-stroke recovery.

Next, we examined the effects of acute ischemic injury on metabolic profiles in 3 month and 12 month old rats. The metabolic responses specific to I/R injury during the early acute phase of reperfusion was dependent on the age of the rats. Younger 3 month rats showed significant changes in the brain but negligible changes in liver. Interestingly, several branched-chain amino acids (BCAAs) and glycine were significantly increased which could potentially contribute to an increase in synthesis of neurotransmitters including glutamate and GABA thereby affecting the brain chemistry and function in the early acute phase of I/R injury (Sapieha et al., 2008). BCAA are also essential amino acids and therefore, are important for protein synthesis. Additionally, glycine is involved in synthesis of DNA, phospholipids, collagen, and production of energy and therefore, may have neuroprotective role (Fernstrom, 2005). An accumulation of these amino acids in the early acute phase may suggest altered neurotransmitter levels and protein synthesis in the brain due to injury. Glutathione was observed to be significantly reduced at this stage in the brain highlighting an increase in reactive oxygen species (ROS), inflammation, and apoptosis that are often seen in post-stroke brain (Allen and Bayraktutan, 2008). Use of anti-inflammatory agents and antioxidants has the potential of reducing inflammation by increasing glutathione levels.

Surprisingly, brain of 12 month rats responded minimally, but significant changes were seen in the liver due to ischemic injury during acute phase of I/R. Particularly, the antioxidant glutathione, was significantly reduced, possibly augmenting oxidative stress that is typically associated with cell death. On the other hand, a ketone body, 3-HB was increased presumably augmenting repair process as it can fulfill energy requirement for the brain. Also, a significant change occurred in taurine, a major bile acid conjugate, suggesting an impairment in liver functioning (Amelio et al., 2014). These changes were accompanied with an increase in creatine which has been shown to reduce the risk of neurological damage following ischemic stroke in mice (Miyazaki and Matsuzaki, 2014). In addition, increased phosphocholine (PC) and decreased levels of specific amino acids including alanine, serine, tyrosine, and tryptophan are likely to affect protein synthesis and energy metabolism, and tip the homeostasis in the liver of aging rats. However, further functional studies are required to elucidate their specific roles in stroke. These metabolic alterations further support the differential tissue responses to stroke due to aging, warranting the use of age appropriate animal models in stroke therapeutic studies.

Next, we found significant alterations in secreted metabolites in plasma. Interestingly, circulating metabolites including citrate and Acetyl-L-carnitine (ALCAR), which can regulate inflammation and fatty acid metabolism, and tyrosine and lysine, which play a role in protein synthesis and neurotransmission. These metabolic changes in plasma indicate an important role in regulating metabolic and physiological pathways during acute phase of stroke, independent of age.

Lastly, we examined the effects of prolonged time of reperfusion on metabolic alterations. Reperfusion time after ischemic injury is an important determinant of post-stroke outcome. Delineating the metabolic consequences of I/R time may lead to better understanding of extended window of opportunity for stroke therapy. Here, we show that local organ brain, and the peripheral organ liver, and blood/plasma show metabolic responses sequentially as a function of reperfusion time, and in a tissue specific manner. Not surprisingly, brain exhibited major metabolic changes during early acute phase in response to I/R injury. In addition several metabolites were altered during an extended period of reperfusion time as shown in Supplementary Table 1. Of note, formate levels remained at a higher levels even after day 3 of I/R, which is consistent with its increased levels in the plasma of stroke patients (Jung et al., 2011).

In the liver, both NAD and NADP levels were significantly reduced, and nucleotide derivatives including uridine and nicotinurate were significantly increased for an extended period of I/R injury, indicating that pyrimidine, nicotinate and nicotinamide metabolism are indeed affected by re-perfusion time. Most importantly, glutathione levels remained low up to week 2 of re-perfusion time, clearly suggesting a gradual increase in oxidative stress in brain during acute phase and then systemically during later repair phase. Creatine alterations followed similar trend as glutathione. These results demonstrate the significant and persistent systemic effects on metabolic pathways due to time of reperfusion.

Secreted metabolites were also affected by the reperfusion time, indicating the gradual effects of brain injury on metabolites in blood and peripheral organ including liver. These specific metabolic signature may provide insight into the identification of potential biomarkers. Indeed, our study revealed citrate, lysine, and tyrosine as putative plasma biomarkers in the acute phase of I/R injury in both younger and older animals. Interestingly, previous study has shown statistically significant reduction in citrate concentration in urine of stroke patients although, its abundance in plasma was below the sensitivity in their experiments (Jung et al., 2011). Further studies are required to validate the relevance of these blood biomarkers in stroke pathology.

5. Conclusions

The findings of this comprehensive study using the rat MCAO stroke model and NMR spectroscopy approach, help us understand differential metabolic changes due to aging process, acute ischemic stroke, and extended reperfusion time. These observations provide broad insight for local and prolonged systemic effects of stroke on metabolism, particularly in brain, liver, and blood plasma. Interestingly, we found that young and older rats respond to stroke in a tissue/organ specific manner pointing to a potential role for not only local, but also systemic

effects of cerebral ischemia. Overall, our studies demonstrate that increasing aging and cerebral ischemia may evoke both specific and common metabolic responses in the post-stroke brain, plasma, and peripheral organ liver. Further studies are however needed to elucidate the metabolic interactions and specific mechanisms underlying the association between systemic organ dysfunction and post-stroke brain repair and recovery.

Acknowledgements

This work was in part supported by the department of Neurological Surgery, UW-Madison, American Heart Association AHA-7GRNT33700105 (UVW), and R01CA164492 (SPP). The Nuclear Magnetic Resonance Facility at UW-Madison is supported by NIH grants P41GM103399 and P41GM66326. Equipment in the facility was purchased with funds from the University of Wisconsin, the NIH (P41GM66326, P41RR02301, P41GM103399, RR02781, RR08438), the NSF (DMB-8415048, OIA-9977486, BIR-9214394), and the U.S. Department of Agriculture.

Appendix A. Supplementary data

Supplementary data to this article can be found online at https://doi.org/10.1016/j.neuint.2019.01.025.

6. Author contributions

U.V.W. developed the conceptual idea of the project, designed and conducted the experiments, and collected the plasma and brain tissue samples, and prepared the manuscript. J.F.H. performed the MCAO surgeries and collected tissues. V.J.B. performed NMR experiments and statistical analysis, and contributed to the preparation of manuscript. R.J.D., and S.P.P. provided overall supervision of the study and reviewed the manuscript. All authors reviewed the manuscript.

Compliance with ethical standards

Disclosures/conflict of interest

All the authors declare that there are no financial or other interests with regard to the submitted manuscript that might be construed as a conflict of interest.

Funding

This work was in part supported by the resources provided by the Department of Neurosurgery, University of Wisconsin, Madison, American Heart Association AHA-7GRNT33700105 (UVW), and NIHR01CA164492 (SPP).

Ethical approval

All animal work was carried out in accordance with the NIH and ARRIVE *Guidelines for the Care and Use of Laboratory Animals*. All animal care and surgical procedures were approved by the Animal Care and Use Committee of the University of Wisconsin-Madison.

This article does not contain any studies with human participants.

Additional information

The raw spectra and processing information along with the quantification summary is uploaded to the MetaboLights server (Xia et al., 2015) (Study ID: MTBLS516).

References

Allen, C.L., Bayraktutan, U., 2008. Risk factors for ischaemic stroke. Int. J. Stroke 3 (2), 105–116.
Amelio, I., Cutruzzolá, F., Antonov, A., et al., 2014. Serine and glycine metabolism in cancer. Trends Biochem. Sci. 39, 191–198.
Bake, S., Okoreeh, A.K., Alaniz, R.C., Sohrabji, F., 2016 Jan. Insulin-like growth factor (IGF)-I modulates endothelial blood-brain barrier function in ischemic middle-aged female rats. Endocrinology 157 (1), 61–69.
Beckonert, O., Keun, H.C., Ebbels, T.M.D., et al., 2007. Metabolic profiling, metabolomic and metabonomic procedures for NMR spectroscopy of urine, plasma, serum and tissue extracts. Nat. Protoc. 2, 2692–2703.
Bhute, V.J., Palecek, S.P., 2015. Metabolic responses induced by DNA damage and poly (ADP-ribose) polymerase (PARP) inhibition in MCF-7 cells. Metabolomics 11, 1779–1791.
Bhute, Vijesh J., Ma, Y., Bao, X., Palecek, S.P., 2016. The poly (ADP-ribose) polymerase inhibitor Veliparib and radiation cause significant cell line dependent metabolic changes in breast cancer cells. Sci. Rep. 6, 36061.
Bhute, Vijesh J., Bao, X., Dunn, K.K., Knutson, K.R., McCurry, E.C., Jin, G., Lee, W.H., Lewis, S., Ikeda, A., Palecek, S.P., 2017. Metabolomics identifies metabolic markers of maturation in human pluripotent stem cell-derived cardiomyocytes. Theranostics 7 (7), 2078.
Braidy, N., Guillemin, G.J., Mansour, H., et al., 2011. Age related changes in NAD+ metabolism oxidative stress and Sirt1 activity in wistar rats. PLoS One 6, e19194.
Cai, W., Zhang, K., Li, P., et al., 2017. Dysfunction of the neurovascular unit in ischemic stroke and neurodegenerative diseases: an aging effect. Ageing Res. Rev. 34, 77–87.
Connolly, G.P., Duley, J.A., 1999. Uridine and its nucleotides: biological actions, therapeutic potentials. Trends Pharmacol. Sci. 20, 218–225.
Coon, A.L., Arias-Mendoza, F., Colby, G.P., et al., 2006. Correlation of cerebral metabolites with functional outcome in experimental primate stroke using in vivo 1H-magnetic resonance spectroscopy. AJNR Am J Neuroradiol 27, 1053–1058.
Dieterle, F., Ross, A., Schlotterbeck, G., et al., 2006. Probabilistic quotient normalization as robust method to account for dilution of complex biological mixtures. Application in 1H NMR metabonomics. Anal. Chem. 78, 4281–4290.
Eun, M.Y., Seo, W.K., Lee, J., Kim, M., Kim, J., Kim, J.H., Oh, K., Koh, S.B., 2013. Age-dependent predictors for recurrent stroke: the paradoxical role of triglycerides. Eur. Neurol. 69 (3), 171–178.
Fernstrom, J.D., 2005. Branched-chain amino acids and brain function. J. Nutr. 135, 1539S–1546S.
Jové, M., Mauri-Capdevila, G., Suárez, I., et al., 2015. Metabolomics predicts stroke recurrence after transient ischemic attack. Neurology 84, 36–45.
Jung, J.Y., Lee, H.-S., Kang, D.-G., et al., 2011. 1H-NMR-based metabolomics study of cerebral infarction. Stroke 42, 1282–1288.
Kelly-Hayes, M., Beiser, A., Kase, C.S., et al., 2003. The influence of gender and age on disability following ischemic stroke: the Framingham study. J. Stroke Cerebrovasc. Dis. 12, 119–126.
Kim, Y., Kim, Y.S., Noh, M.-Y., et al., 2017. Neuroprotective effects of a novel poly (ADP-ribose) polymerase-1 inhibitor, JPI-289, in hypoxic rat cortical neurons. Clin. Exp. Pharmacol. Physiol. 44, 671–679.
Luo, L., Zhen, L., Xu, Y., et al., 2016. (1)H NMR-based metabonomics revealed protective effect of Naodesheng bioactive extract on ischemic stroke rats. J. Ethnopharmacol. 186, 257–269.
Ma, Y., Chen, H., He, X., et al., 2012. NAD+ metabolism and NAD(+)-dependent enzymes: promising therapeutic targets for neurological diseases. Curr. Drug Targets 13, 222–229.
Ma, S., Zhao, H., Ji, X., et al., 2015. Peripheral to central: organ interactions in stroke pathophysiology. Exp. Neurol. 272, 41–49.
Massudi, H., Grant, R., Braidy, N., et al., 2012. Age-associated changes in oxidative stress and NAD+ metabolism in human tissue. PLoS One 7, e42357.
Mauri-Capdevila, G., Jove, M., Suarez-Luis, I., et al., 2013. Metabolomics in ischaemic stroke, new diagnostic and prognostic biomarkers. Rev. Neurol. 57, 29–36.
Miyazaki, T., Matsuzaki, Y., 2014. Taurine and liver diseases: a focus on the heterogeneous protective properties of taurine. Amino Acids 46, 101–110.
Moskowitz, M.A., Lo, E.H., Iadecola, C., 2010. The science of stroke: mechanisms in search of treatments. Neuron 67, 181–198.
Mozaffarian D, Benjamin EJ, Go AS, et al.. Executive summary: Heart disease and stroke statistics—2016 update. Circulation; 133.
Muscari, A., Collini, A., Fabbri, E., et al., 2014. Changes of liver enzymes and bilirubin during ischemic stroke: mechanisms and possible significance. BMC Neurol. 14, 122.
Nagana Gowda, G. a., Raftery, D., 2014. Quantitating metabolites in protein precipitated serum using NMR spectroscopy. Anal. Chem. 86, 5433–5440.
Ponzio, F., Calderini, G., Lomuscio, G., et al., 1982. Changes in monamines and their metabolite levels in some brain regions of aged rats. Neurobiol. Aging 3, 23–29.
Purroy, F., Cambray, S., Mauri-Capdevila, G., et al., 2016. Metabolomics predicts neuroimaging characteristics of transient ischemic attack patients. EBioMedicine 14, 131–138.
Sapieha, P., Sirinyan, M., Hamel, D., et al., 2008. The succinate receptor GPR91 in neurons has a major role in retinal angiogenesis. Nat. Med. 14, 1067–1076.
Schicho, R., Shaykhutdinov, R., Ngo, J., et al., 2012. Quantitative metabolomic profiling of serum, plasma, and urine by (1)H NMR spectroscopy discriminates between patients with inflammatory bowel disease and healthy individuals. J. Proteome Res. 11, 3344–3357.
Schmued, L.C., Hopkins, K.J., 2000. Fluoro-Jade B: a high affinity fluorescent marker for the localization of neuronal degeneration. Brain Res. 874, 123–130.
Simpkins, J.W., Mueller, G.P., Huang, H.H., et al., 1977. Evidence for depressed

catecholamine and enhanced serotonin metabolism in aging male rats: possible relation to gondotropin secretion. Endocrinology 100, 1672–1678.
Wang, R.-Y., Wang, P., Yang, Y.R., 2003. Effect of age in rats following middle cerebral artery occlusion. Gerontology 49, 27–32.
Wen, S.W., Wong, C.H.Y., 2017. An unexplored brain-gut microbiota axis in stroke. Gut Microb. 1–6.
Wesley, U.V., Hatcher, J.F., Ayvaci, E.R., et al., 2017. Regulation of dipeptidyl peptidase IV in the post-stroke rat brain and in vitro ischemia: implications for chemokine-mediated neural progenitor cell migration and angiogenesis. Mol. Neurobiol. 54, 4973–4985.
Wolahan, S.M., Hirt, D.G.T., 2015. Translational metabolomics of head injury: exploring dysfunctional cerebral metabolism with ex vivo NMR spectroscopy-based metabolite quantification. In: Kobeissy, F.H. (Ed.), Brain Neurotrauma: Molecular, Neuropsychological, and Rehabilitation Aspects. CRC Press/Taylor & Francis, Boca Raton (FL).
Xia, J., Sinelnikov, I.V., Han, B., et al., 2015. MetaboAnalyst 3.0–making metabolomics more meaningful. Nucleic Acids Res. 1–7.
Ye, Ruidong, Shi, Ming, Liu, Qian, Chen, Jieli, 2016. Redox imbalance and stroke. Oxid Med Cell Longev 2016, 3065263.